The centrosomal Deubiquitylase USP21 regulates Gli1 transcriptional activity and stability.

Claire Heride[§], Daniel J. Rigden[¶], Erithelgi Bertsoulaki[§], Danilo Cucchi [$], Enrico De Smaele [#], Michael J. Clague[§], Sylvie Urbé[§]

[§]Cellular and Molecular Physiology, Institute of Translational Medicine, University of Liverpool, Crown Street, Liverpool L69 3BX, UK
[¶]Institute of Integrative Biology, University of Liverpool, Liverpool L69 7ZB, United Kingdom
[#]Department of Experimental Medicine, Sapienza University of Rome, Rome, Italy
[$]Department of Molecular Medicine, Sapienza University of Rome, Italy

Running Title: USP21 regulates Hedgehog signalling

Keywords: Ubiquitin, Hedgehog, Gli1, PKA, phosphorylation, DUB

Summary statement:

We identify a Hedgehog pathway associated ubiquitin ligase adapter as a direct interaction partner of the deubiquitylase USP21 and discover a close interplay between USP21 and PKA in regulating Gli1.

Abstract

USP21 is a centrosome-associated deubiquitylase (DUB) that has been implicated in the formation of primary cilia, critical organelles for the regulation of the Hedgehog (Hh) signaling pathway in vertebrates. Here we identify KCTD6, a Cullin3 E3-ligase substrate adapter previously linked to Hh-signaling, as well as Gli1, the key transcription factor responsible for Hh signal amplification, as novel interacting partners of USP21. We identify a cryptic structured protein interaction domain in KCTD6, which is predicted to bear fold similarity to Smr domains. Importantly, we show that both depletion and overexpression of catalytically active USP21 suppress Gli1-dependent transcription. Gli-proteins are negatively regulated through PKA-dependent phosphorylation. We provide evidence that USP21 recruits and stabilises Gli1 at the centrosome where it promotes its phosphorylation by PKA. By revealing an intriguing functional pairing between a spatially restricted DUB and a kinase, our study highlights the centrosome as an important hub for signal coordination.

INTRODUCTION

Hedgehog (Hh) signaling plays an important role during development and has also been implicated in diverse malignancies including basal cell carcinomas, medullo- and glioblastoma, as well as pancreatic, colon and breast carcinomas (Amakye et al., 2013; Takebe et al., 2015). Inhibitors of this pathway are under assessment in the clinic as potential anti-cancer therapeutics (Gonnissen et al., 2015; Takebe et al., 2015). The general architecture of the pathway was initially discovered in Drosophila (Nusslein-Volhard and Wieschaus, 1980) but much of the cascade is highly conserved from flies to vertebrates (Briscoe and Therond, 2013; Ingham et al., 2011). In contrast to many other signaling pathways, Hh signaling is constitutively repressed by the interplay of two multi-spanning transmembrane proteins, Patched (PTC in Drosophila, PTCH1 and 2 in mammals) and Smoothened (SMO). In the absence of a signal, PTC/PTCH1/2 inhibit SMO, and the key transcription factors, Ci (Cubitus interruptus) in Drosophila and Gli2/3 in mammals, are converted to transcriptional repressors. Gli2/3 are phosphorylated by a series of kinases (PKA, CK1, GSK3ß) and in particular Gli3 undergoes processing (limited proteolysis) in a phosphorylation, ubiquitylation and proteasome dependent manner

to a transcriptionally repressive form. Activation of the pathway is triggered by binding of Hh ligands to PTCH1/2, which triggers their endocytosis and leads to de-repression of SMO favouring activation of Ci/Gli proteins. These translocate into the nucleus and activate expression of Hh-responsive genes (Hui and Angers, 2011). In mammalian cells, activation of the cascade is localised at the primary cilium, a specialised, microtubule based surface organelle. Release of SMO inhibition leads to SMO, Gli2 and Gli3 translocation to the cilium and subsequent translocation of the unprocessed transcriptionally active Gli proteins to the nucleus. One of the transcriptional targets is Gli1, which exclusively functions as an activator of the cascade. It is the balance of active and repressive Gli-proteins that determines signal strength and outcome.

Post-translational modifications play key roles in this cascade (Chen and Jiang, 2013; Gulino et al., 2012). Reversible ubiquitylation can either promote protein degradation or alter subcellular localisation or activity of a protein. Multiple E3-ligases are thought to play critical roles in Hh signaling: Cullin1-Slimb/βTrCP, Cullin3-HIB-Roadkill/SPOP and Itch have all been shown to ubiquitylate and destabilise Gli proteins (Jiang, 2006). Approximately 90 deubiquitylases (DUBs) are encoded in the human genome (Clague et al., 2013; Komander et al., 2009). This family of enzymes has been implicated in the regulation of many canonical signal transduction cascades, e.g. NFkB, Wnt, TGFß and the Ras-MAPK pathway (Clague et al., 2012a; Hayes et al., 2012; Keusekotten et al., 2013). USP8 has been associated with this cascade in Drosophila, where it promotes recycling of SMO (Clague et al., 2012b; Li et al., 2012; Xia et al., 2012). However, the role of DUBs in the mammalian Hh signaling pathway has only recently been explored (Zhou et al., 2015).

We have previously characterised USP21 as the only centrosome and microtubule associated DUB in a comprehensive localisation screen (Urbe et al., 2012). USP21 also associates with basal bodies in ciliated cells and its depletion inhibits the formation of primary cilia, which play a critical role in the initiation of Hh signaling in vertebrates. Here we identify a novel binding partner of USP21, the BTB-domain containing, Cullin E3 ligase adapter protein KCTD6 (KCASH3), which has previously been implicated in Hh signaling (De Smaele et al., 2011). Importantly, we go on to show that either depletion or overexpression of USP21 suppresses Gli1-dependent transcription in human cells. Our results reveal that USP21 stabilises Gli1

at the centrosome and promotes its phosphorylation by PKA, thus contributing to the intricate compartmentalisation of the Hh signaling pathway.

RESULTS

Identification of novel USP21 interacting partners

We have used a Yeast-two-hybrid (Y2H) approach to search for direct interactors of USP21 that may act as substrates or substrate adaptors in the context of microtubule- and centrosome-dependent processes. Out of a panel of USP21 fragments, only those encompassing amino acids [1-174] and [Δ1-47] passed the suitability test by failing to auto-activate reporter genes (Materials and Methods, and data not shown). We selected USP21 [Δ1-47], which retains all microtubule binding and centrosome localisation determinants (Urbe et al., 2012), as a bait to screen a universal, normalised human cDNA Y2H library (Fig. 1A). Seven out of ten isolated diploid colonies contained plasmids with in-frame annotated coding sequences, two of which encode ZNF350 (Zinc finger protein 350). The other proteins identified were KCTD6 (BTB/POZ domain-containing protein 6), WDR47 (WD repeat containing protein 47), SYNE1 (Spectrin repeat containing, nuclear envelope 1), MPP1 (Membrane protein, palmitoylated 1, 55kDa) and ANKRD32 (Ankyrin repeat domain containing protein 32) (Table 1, Fig. 1A).

USP21 associates with the BTB-domain protein KCTD6

Two of the six novel USP21 interactors have been shown to localise to microtubule-based structures. WDR47/Nemitin colocalises with cytoplasmic microtubules via its interaction with Microtubule Associated Protein (MAP) 8 (Wang et al., 2012a), whilst MPP1 has been localised to the basal body and the ciliary axoneme in murine photoreceptors (Gosens et al., 2007). We were particularly intrigued by KCTD6, a BTB-domain containing protein that was previously shown to modulate Hedgehog signaling in association with the related KCTD11 (De Smaele et al., 2011). We validated this interaction by co-immunoprecipitation of epitope-tagged proteins from HEK293T cells (Fig. 1B). KCTD6 interacts preferentially with catalytically inactive USP21-C221S (USP21CS), which in turn isolates higher molecular weight species of mono- and di-ubiquitylated KCTD6 (Fig. 1B,C). USP21CS itself presents as a doublet, a phenomenon commonly observed for catalytically inactive mutants of the USP

family, e.g. USP4 and USP15, which tend to accumulate as a mono- and poly-ubiquitylated species (Fig. 1D; (Hayes et al., 2012)).

USP21 interacts with CUL3 via the BTB domain protein KCTD6

KCTD6 binds to Cullin 3 (CUL3) via its BTB domain, suggesting that it acts as a classic substrate adapter of a BTB-CUL3-Rbx1 ubiquitin E3 ligase (De Smaele et al., 2011; Lange et al., 2012; Smaldone et al., 2015). We wondered whether USP21 interacts with a fully assembled KCTD6-CUL3 ligase complex. Interactions between DUBs and E3 ligases are established in the literature but few examples have been analysed in detail (Hayes et al., 2012; Keusekotten et al., 2013; Komander et al., 2009; Schulein-Volk et al., 2014; Sowa et al., 2009; Villeneuve et al., 2013). Both active and inactive USP21 coimmunoprecipitate with CUL3 and vice-versa (Fig. 2B, Fig. S1B). Intriguingly, inactive USP21CS enriches a higher molecular weight species of CUL3 that could in principle correspond to neddylation, which is required for Cullin-Ring ligase activation (Bennett et al., 2010). The Nedd8 Activating Enzyme (NAE) inhibitor MLN4924 did not affect association of Flag-KCTD6 with endogenous CUL3, nor the amount of USP21 bound to KCTD6 (Fig. S1A). Importantly, the supplemental CUL3 band was insensitive to MLN4924 suggesting USP21CS promotes the stabilisation of ubiquitylated forms of both KCTD6 and CUL3 (Fig. S1B).

The interaction between USP21 and CUL3 is most likely indirect and mediated through KCTD6 as a functional BTB-domain is both required and sufficient (Fig. 2A,C-D). Two closely related KCTD family members have also been implicated in Hh signaling (Canettieri et al., 2010). The KCTD6-interactor KCTD11 (KCASH1/REN), but not KCTD21 (KCASH2), binds weakly to wild-type and strongly to catalytically inactive USP21 (Fig. S1C). However, in contrast to KCTD6, KCTD11 does not appear to be modified in GFP-USP21CS coimmunoprecipitates.

Identification of a cryptic protein interaction domain in KCTD6

The best-characterised BTB-domain CUL3 adaptors contain defined substrate interaction domains such as Kelch, MATH, PHR or zinc fingers (Stogios et al., 2005). No such domains have been described for KCTD proteins, yet the region [114-237], directly C-terminal of the BTB domain of KCTD6 is sufficient for interaction with USP21 (Fig. 3A). The combined results of Y2H and pull-down narrow down the USP21 binding site to the [114-187] region of KCTD6 (Fig. 3E). We hypothesized

that this region may contain a cryptic protein interacting domain.

Sensitive bioinformatics tools for detecting distant homologies (HHpred (Soding, 2005)) and the Metaserver for fold recognition (Bujnicki et al., 2001) failed to identify recognisable relatives of the KCTD6 C-terminal domain. Nevertheless, the region is rich in predicted secondary structure, suggestive of a well-folded domain. In favourable cases, *ab initio* modelling can accurately predict the overall fold of a queried protein through stitching together fragments of unrelated proteins (Rohl et al., 2004; Xu and Zhang, 2012). Using this approach, the most promising results were obtained for a region comprising residues [109-213], eliminating 24 residues from the C-terminus that some methods suggest might be intrinsically disordered. QUARK's favoured model bears a striking resemblance to the C-terminal Smr domain of human NEDD4-binding protein 2, with a *Z*-score of 7.1 for the match, well above the threshold of 2 generally taken as indicating significance (PDB code 2vkc (Diercks et al., 2008), Fig. 3B, Fig. S1D). According to this model, the C-terminal section [188-213] of this Smr-like (SmrL) domain, containing a helix and a short ß-hairpin, is separate from the remainder of the structure, which thus might be able to fold independently. Indeed, separate *ab initio* modelling efforts with a shorter stretch comprising residues [109-187] produced results including structures similar to the modelled SmrL domain (not shown). This may account for the observed association of USP21 with a C-terminally truncated KCTD6 [114-187] in our Y2H screen.

Conversely the [Δ1-184] fragment, encompassing the catalytic domain of USP21, is necessary and sufficient to bind KCTD6 as well as CUL3 (Fig. 3C,D). Taken together, our data indicate that CUL3, KCTD6 and USP21 can form a trimeric complex in which the catalytic domain of USP21 interacts with the C-terminal cryptic SmrL-domain of KCTD6, whilst the latter's BTB domain mediates interaction with CUL3 (Fig. 3E).

USP21 does not affect KCTD6 and CUL3 protein levels

Based on previously described interactions between DUBs and E3 ligases, we wondered whether USP21 might either stabilise or modulate the activity of the KCTD6-CUL3-E3 ligase complex. Neither siRNA mediated depletion, nor overexpression of USP21 altered overall CUL3 protein levels or the distribution between active (neddylated) and inactive (non-neddylated) forms (Fig. S2A,B). Unfortunately, none of the commercially available anti-KCTD6 antibodies we tested

recognised endogenous levels of the protein. Flag-KCTD6 protein levels were not significantly affected by overexpression of USP21 (Fig. 1B). We conclude that despite the enrichment of ubiquitylated KCTD6 and CUL3 in USP21CS immunoprecipitates, the stability of either protein is not regulated by USP21. The steady state protein levels of the sole known substrate of the previously described hetero-dimeric KCTD6-KCTD11 CUL3 E3-Ligase, HDAC1, were also unaffected by depletion or overexpression of USP21 (Fig. S2C,D).

USP21 regulates the Hedgehog signaling pathway and modulates Gli1 transcriptional activity

KCTD6 has been proposed to act as a negative regulator of the Hh signaling pathway (De Smaele et al., 2011). We have previously shown that USP21 depletion inhibits the formation of the primary cilium, which also plays a key role in Hh pathway activation in non-transformed cells. In order to assess a potential role of USP21 in Hh signaling, we first measured Gli1 mRNA levels as a transcriptional readout in NIH3T3 cells stimulated with a Smoothened agonist (SAG) (Chen et al., 2002). Depletion of USP21 inhibits SAG-dependent accumulation of endogenous Gli1 mRNA levels (Fig. 4A).

The main transcriptional activator in the pathway is Gli1 itself, which operates via a positive auto-regulatory feedback loop (Hui and Angers, 2011). KCTD6, in concert with KCTD11, has previously been shown to target HDAC1 for ubiquitin-dependent degradation, thereby indirectly modulating the acetylation status and thus transcriptional activity of Gli1. With that in mind, we wanted to assess the ability of USP21 to affect Gli1 transcriptional activity in the absence of extrinsic pathway activation using a Gli1-dependent dual luciferase reporter gene assay. We opted for a heterologuous co-expression system of HA-Gli1 and GFP-USP21 in HEK293T cells, which permit high levels of transfection efficiency. Importantly, this approach introduces constitutively expressed Gli1 together with the Gli1-dependent reporter construct into the cells. This allows us to pinpoint the stage at which USP21 may regulate Hh signaling, downstream of Smo activation, ie downstream of the already established role in primary cilium formation. In this assay, siRNA-mediated depletion of USP21 decreased Gli1 transcriptional activity by 39.8 ± 2.7% (Fig. 4B). Likewise, overexpression of GFP-USP21 inhibits Gli1 transcriptional activity to a similar degree and this inhibition depends on its catalytic activity (Fig. 4C)**.** Altogether these data

indicate that USP21 regulates the Hh signaling pathway and either directly or indirectly modulates Gli1 transcriptional activity.

USP21 interacts with and stabilises Gli1

We wondered whether USP21 might regulate the stability of Gli1 and turned to CRISPR/CAS9 technology to knock-out USP21 in HEK293T cells, which like many cancer cells show autonomous expression of Gli1 (Figure S3A, (Dahmane et al., 1997; Kinzler et al., 1987; Mazza et al., 2013; Nolan-Stevaux et al., 2009; Tariki et al., 2014). Transient transfection with plasmids encoding both CAS9-GFP and either one of five distinct gRNAs, targeting the second exon encompassing the start codon of all annotated USP21 isoforms, resulted in a clear decrease of Gli1 protein levels by 25-50% (Fig. 5A). Note that in this configuration, residual USP21 derives from non-transfected cells. Although these results suggest that USP21 stabilises Gli1, the observed decrease in endogenous Gli1 could in principle reflect transcriptional suppression (see also Fig. 4A).

We next coexpressed HA-tagged Gli1 together with GFP-USP21 and fragments thereof in HEK293T cells. We observed a clear increase in Gli1 protein levels in cells co-expressing full-length USP21 (Fig. 5B and S3B). In order to assess a potential interaction between these two proteins, we immunoprecipitated HA-Gli1 and probed for associated GFP-USP21. Full-length GFP-USP21, but not the shortest N-terminal fragments [1-120; 1-174], was able to associate with Gli1 (Fig. 5C). Both the unstructured N-terminal [1-210] region, required for microtubule and centrosome association, and the C-terminal USP21 [Δ1-184] region, harbouring the catalytic domain, were capable of binding Gli1 independently of each other. Likewise, Flag-tagged Gli1 and Gli2 were able to co-precipitate Myc-tagged USP21 from HEK293T cells (Fig. S3C-D).

Having shown above that the catalytic domain of USP21 also interacts with the KCTD6-CUL3 E3-ligase complex, we wondered whether KCTD6 would be able to influence Gli1 stability in this setting. Co-expression of KCTD6 with USP21 counteracts its ability to stabilise Gli1 (Fig. 5D). This suggests the direct interaction of KCTD6 with the USP21 catalytic domain disrupts its regulation of Gli1.

USP21 stabilises a phosphorylated form of Gli1

The increase of Gli1 protein levels upon USP21 overexpression appears to be at odds with the observed inhibition of Gli1-transcriptional activity in this setting (Fig. 4C). On close inspection, we observed a higher molecular weight form of Gli1 in USP21 overexpressing cells, indicative of a post-translational modification (Fig. 6A). This band was significantly reduced in cells coexpressing catalytically inactive USP21CS, and absent in cells expressing truncated versions of USP21 (Fig. S3B). Many components of the Hh signaling pathway are regulated by acetylation, phosphorylation, ubiquitylation and sumoylation (Chen and Jiang, 2013; Gulino et al., 2012). In particular, Gli transcriptional activity is regulated by several kinases, thus we assessed whether USP21 induces Gli1 phosphorylation. Incubation of immunoprecipitated HA-Gli1 with Calf Intestinal Alkaline Phosphatase (CIP) induced the disappearance of the upper band that is only present in cells overexpressing full-length USP21 (Fig. 6B).

Phosphorylation of Gli transcription factors can either activate or inhibit their transcriptional activity. In the absence of pathway activation, sequential phosphorylation of Gli3, and to a lesser extent Gli2, by PKA, CKI and GSK3β induces ubiquitin-dependent limited proteolysis to generate a transcriptionally repressive form, GliR (Briscoe and Therond, 2013; Hui and Angers, 2011). Phosphorylation by PKA alone leads to Gli2/3 inactivation (Niewiadomski et al., 2014; Tuson et al., 2011) and has been proposed to inhibit nuclear localisation of Gli1 (Sheng et al., 2006). Finally, phosphorylation of Gli1 by S6K1 in response to mTOR activation triggers its release from the repressor SuFu leading to its transcriptional activation (Wang et al., 2012b). Guided by our functional experiments indicating an inhibitory role of USP21 expression on Gli1-dependent transcription (Fig. 4C), we focused on PKA-dependent phosphorylation as a potential target of USP21. Co-expression of PKI, a well-established PKA-inhibitor (Scott et al., 1985), abolished the USP21-induced accumulation of phosphorylated Gli1 (Fig. 6C). Strikingly, the decrease of Gli1 phosphorylation is concomitant with a decrease in its protein levels, suggesting that USP21 induced phosphorylation of Gli1 is coupled with its stabilisation (Fig. 6C). Similarly, a pool of Gli2 appears stabilised in a PKI-sensitive manner by co-expression of USP21 (Figure S3C-D and S4A). Altogether these data indicate that USP21 stabilises inactive Gli1 and promotes its phosphorylation by PKA.

USP21 promotes Gli1 localisation at the centrosome

How then could the deubiquitylase USP21 induce Gli1 phosphorylation by PKA? We have previously reported that USP21 is most highly enriched at the centrosome and basal body of ciliated cells (Urbe et al., 2012). PKA has previously been shown to be enriched and active at these two locations (Nigg et al., 1985; Terrin et al., 2012; Tuson et al., 2011). U2OS cells allow ready discrimination of intracellular structures due to their planar geometry and expanded cytoplasm. In these cells, endogenous PKA colocalises with GFP-USP21 at the centrosome (Fig. 6D). Neither wild-type or catalytically inactive USP21 affect PKA protein levels (Fig. S4B). Given that full stabilisation of phosphorylated Gli1 requires the USP21 N-terminal microtubule and centrosome targeting sequence, we wondered whether USP21 influences the localisation of Gli1. Expressed on its own, HA-Gli1 presents with a diffuse, cytoplasmic and nucleoplasmic staining. However, co-expression of either wild-type or catalytically inactive GFP-USP21 strongly promotes its recruitment to the centrosome (Fig. 6E).

DISCUSSION

USP21 interacts with KCTD6, a CUL3 substrate adapter via its catalytic domain

Our genome wide Y2H screen has yielded six novel interactors of USP21. The fact that WDR47 and MPP1 have been shown to associate with microtubules or the basal body and axoneme, respectively, makes these likely candidates for future studies (Gosens et al., 2007; Wang et al., 2012a). Here, we have focused exclusively on KCTD6, a CUL3-binding BTB protein that has previously been implicated in the Hh signaling pathway. This pathway is of particular interest to USP21 function, due to its prominent association with centrosomes, basal bodies, microtubules and primary cilia. We have mapped this interaction to the catalytic domain of USP21 and a novel cryptic protein interaction domain, here called Smr-like (SmrL) that is unique to KCTD6. The Smr domain is generally associated with nuclease function (Fukui et al., 2007). However the KCTD6-SmrL does not bear the positively charged surface of the NEDD4BP2 Smr structure characteristic of DNA/RNA binding proteins, nor a suitably positioned catalytic Glu residue (Zhang et al., 2014). Browsing the SCOP structure classification database (Andreeva et al., 2008) at the fold level containing Smr domains reveals a second theme of protein-protein interaction, exemplified by bacterial sulphurtransferase TusA (Shi et al., 2010) and the predicted dimeric form of NEDD4BP2 (according to the PISA resource (Krissinel and Henrick, 2007)). This is clearly consistent with the protein-protein interaction role determined here for the KCTD6 C-terminal domain and supported by existing precedents of the same fold serving both DNA- and protein-binding functions (cf zinc fingers (Matthews and Sunde, 2002)). The novel SmrL domain is restricted to KCTD6, although KCTD11 and 21 may harbor their own distinct cryptic domains adjacent to the BTB. KCTD11, but not KCTD21, has been shown to hetero-dimerise with KCTD6, providing a possible explanation for its interaction with USP21 in pull-down experiments. USP21, unlike many other members of the USP family, does not contain insertions in its catalytic domain that may encode additional protein interaction motifs or domains. Thus, KCTD6 is the first protein besides Ubiquitin (and ISG15 (Ye et al., 2011)) that interacts with the catalytic core of USP21, and a rare example of a core binding protein considering the USP family as a whole.

What then is the role of this interaction? E3-ligase DUB interactions can protect the ligases from autoubiquitylation (e.g. MDM2 stabilisation by USP7

(Cummins and Vogelstein, 2004), BRAP/IMP stabilisation by USP15 (Hayes et al., 2012)). Alternatively they may limit the levels of the respective DUBs or exert fine control over a common substrate. We have not found evidence that USP21 and KCTD6 affect each other's stability, nor does USP21 affect global CUL3 stability or neddylation status. However, the fact that co-expression of catalytically inactive USP21 results in the accumulation of minor mono- and di-ubiquitylated species of KCTD6 and CUL3, indicates the potential for USP21 to modulate their ubiquitylation status. Alternatively, USP21 may be acting directly to deubiquitylate the substrates of the Cullin Ring Ligase, in an analogous fashion to USP28, which associates with the CUL1-adapter FBW7 to deubiquitylate a range of substrates including MYC (Schulein-Volk et al., 2014). In contrast to FBW7, we have very little knowledge of the substrates targeted by KCTD6. The closely related BTB-proteins KCTD11 and KCTD21 undergo hetero and homo-dimerisation to target HDAC1 for CUL3-dependent ubiquitylation and degradation (Canettieri et al., 2010). Degradation of HDAC1 promotes the accumulation of transcriptionally inactive, acetylated Gli1. De Smaele and colleagues reported that KCTD6, despite lacking a binding site for HDAC1, could dimerise with its paralogues KCTD11 (but not KCTD21) and contribute to HDAC1 ubiquitylation and degradation (De Smaele et al., 2011). Whilst we cannot exclude that USP21 directly stabilises KCTD6 substrates, we have not observed any global effects on HDAC1 protein levels in response to siRNA mediated depletion or overexpression of USP21.

USP21, a novel regulator of the Hh signaling pathway

Our results suggest that endogenous USP21 positively regulates Hh signaling by two independent mechanisms: Firstly, we have previously shown that USP21 depletion interferes with the formation of primary cilia, the specialised organelles that host the initiation of the Hh signaling cascade in untransformed mammalian cells (Goetz and Anderson, 2010; Urbe et al., 2012). Secondly, we now show that depletion of USP21 not only inhibits SAG-induced transcription in ciliated NIH3T3 cells but also directly interferes with Gli1-dependent activation of a Gli-promoter driven luciferase reporter in Gli1-transfected HEK293T cells. AlthoughHEK293T cells have previously been shown to be capable of generating primary cilia (Gerdes et al., 2007; Lancaster et al., 2011), under the conditions of our assay (48 hrs in 0.5% FBS) only 30% of cells do so. Whilst we cannot exclude that some aspects of exogenous

Gli1-activation may rely on primary cilium formation, taken together our data showing 1) an interaction between USP21 and Gli1, 2) the regulation of PKA dependent phosphorylation of Gli1 by USP21, and 3) the colocalisation of all three proteins at the centrosome in U2OS cells make a strong case for a regulatory role of USP21 that may be independent of cilium formation.

This positions USP21 downstream of SMO and PTCH, and highlights its potential as a new drug target to counteract Hh signaling. This may be of particular relevance in tumours expressing aberrant levels of Gli1 or that are otherwise activated downstream of PTCH and thus resistant to the SMO-inhibitor Vismodegib (Amakye et al., 2013). In this context it is interesting to note that USP21 has been identified in a large-scale screen as one of only few genes with a significantly increased copy number count in breast tumour samples (Kan et al., 2010). The fact that both depletion and overexpression of USP21 interfere with Gli1-dependent transcription suggests that appropriate USP21 protein levels are key to ensure optimal Hh signaling outputs.

Dual role of USP21 in stabilising phosphorylated Gli1 at the centrosome

Intriguingly, overexpression of USP21 represses Gli1-dependent transcription despite the fact that the total amount of Gli1 is clearly increased. Associated with this, we observe the accumulation of a phosphorylated pool of Gli1 in USP21 overexpressing cells. Whilst we have not identified the phosphorylation sites in this study, we provide evidence for the kinase involved in this modification. PKA has recently been shown to phosphorylate multiple serines that are conserved in all Gli-proteins and to suppress Gli-activity in the absence of a Hh signal (Niewiadomski et al., 2014). Our results suggest that USP21 overexpression facilitates these phosphorylation events by recruiting Gli1 either directly or indirectly to the centrosome, which harbours active PKA (Terrin et al., 2012). In ciliated cells, USP21 is localized at the centrosome-derived basal body, where PKA is thought to act on Gli proteins travelling to and from the cilium (Tuson et al., 2011). USP21 may thus promote coincidence of substrate and kinase at these locations. Our data suggest that expression levels of USP21 need to be tightly regulated as both its depletion and overexpression can hamper Hh signaling. However, the role of USP21 exceeds that of an adapter, since both localisation determinants and catalytic activity are required for maximal stabilisation of phosphorylated Gli1 (Fig. 5B and Fig. S3A). It is

conceivable that USP21 regulates both the phosphorylation status and the stability of Gli1 (and possibly Gli2) at the centrosome (Fig. 6F). Our finding provides a unique illustration of the close interplay of a DUB and a kinase at this location and supports the concept of centrosomes functioning as intracellular signaling hubs/scaffolds (Arquint et al., 2014).

A recent report has identified USP7 as a DUB that is able to stabilise Gli2/3 by opposing both Ubiquitin E3-ligase complexes involved in processing or degradation of Gli2/3 in the absence or presence of Hh, SCF(ßTRCP) (Slmb/Cul1) and Itch (HIB/CUL3) respectively (Zhou et al., 2015). Our results suggest a more complex scenario in which the restricted localisation of USP21 facilitates the accumulation of an inactive pool of Gli1 at the centrosome. Extending this model to the basal body provides a means of orchestrating Gli protein activity upon entry into or exit from the primary cilium.

MATERIALS AND METHODS

Yeast-two-hybrid - The coding sequences for USP21[Δ1-47] was subcloned from pCR4-TOPO-USP21[Δ1-47] into the pGBKT7 vector (Clontech). The resultant pGBKT7-USP21[Δ1-47] plasmid was sequenced-verified and transformed into Y2HGold yeast cells. Single colonies that failed to autonomously activate the reporter genes in the absence of prey proteins on -Tryptophan/X-alpha-Gal plates, -Tryptophan/X-alpha-Gal/AureobasidinA plates and -Tryptophan/-Adenine/-Histidine/X-alpha-Gal/AureobasidinA plates were selected for the mating procedure. Briefly, Y2HGold pGBKT7-USP21[Δ1-47] cells were incubated with the human normalised cDNA Y187 prey library (Clontech) in 2YPAD for 23h at 30°C. More than $2.4x10^6$ diploid clones were screened and selected for 5 days on SD/-Trp/-Leu/X-α-Gal/Aba. 20 clones were picked and streaked onto SD/-Trp/-Leu/-His/-Ade/X-α-Gal/Aba plates for 7 days. Interacting proteins were identified by yeast colony PCR and subsequently by sequencing of the extracted plasmid.

Cell culture and transfection – U2OS, HEK293T and NIH3T3 cells were cultured in Dulbecco's modified Eagle medium (DMEM) with Glutamax (Gibco, Carlsbac, CA). Media were supplemented with 10% FBS, 1% nonessential amino acids solution, and 1% penicillin/streptomycin. All cell lines are routinely tested for mycoplasma

contaminations. Transfections of plasmids in HEK293T and U2OS cells were performed with Genejuice (Novagen). For the dual luciferase reporter assays (Promega), plasmids were transfected with lipofectamine 2000 (Invitrogen) into HEK293T cells (DMEM, 0.5%FBS). Cells were fixed or lysed 24h after transfection. For siRNA experiments, cells were treated with non-targeting (NT3) or target specific siRNA oligos (Dharmacon On Target Plus oligos, Thermo Fisher Scientific; Supplementary Table 1) at 40nM final concentration, once or twice over a period of 96h (HEK293T) or 120h (U2OS). NIH3T3 cells were treated at 12nM final concentration, twice over a period of 120h. All siRNA experiments were performed using RNAiMAX (Invitrogen). For Hh pathway activation, the NIH3T3 cells were first serum starved in DMEM with Glutamax for 24h, prior to addition of 100nM SAG or DMSO for 4h.

Quantitative reverse transcription-PCR (RT-PCR) - Cells were lysed and mRNA extracted using the RNAeasy mini kit (Qiagen). cDNA synthesis was performed using 1μg RNA with RevertAid H-minus M-MuLV reverse transcriptase (Fermentas) using an oligo-dT primer (Promega). Quantitative real-time RT-PCR was performed in triplicate using iTaq Universal SYBR Green Supermix and a CFX Connect Real-Time PCR detection machine (Bio-Rad). Primer sequences are listed in the Supplementary table 2.

Co-immunoprecipitation - HEK293T cells were transfected with a total of 2.4μg of DNA per $1x10^6$ cells. 24h after transfection, the cells were washed in cold phosphate-buffered saline (PBS) and lysed in RIPA-lysis buffer (10mM Tris-HCl pH7.5, 150mM NaCl, 1% NP40, 0.1% SDS, 1% sodium deoxycholate) or in NP40-lysis buffer (0.5% NP40, 25mM Tris-HCl pH7.5, 100mM NaCl, 50mM NaF) supplemented with 10mM N-Ethylmaleimide and mammalian protease inhibitor (Sigma) and phosphatase inhibitor cocktails (Roche). Lysates were incubated with primary antibodies and protein G or protein A-agarose beads (P4691 and P2670, Sigma) or with anti-FLAG M2 Affinity Gel (Sigma, A2220) for 1h at 4°C. Beads were washed with RIPA or YP-IP buffer (0.1% NP40, 25mM Tris pH7.5 and 150mM NaCl) 3-5 times and once with 10mM Tris pH7.5. Immunoprecipitated samples and 10μg of the input were evaluated by western blotting.

Western blot analysis - Cultured cells were lysed with RIPA or NP40-lysis buffers (see above). Proteins were resolved by SDS PAGE (Invitrogen NuPage gel 4-12%), transferred to nitrocellulose and probed with primary antibodies over night. For anti-ubiquitin antibodies, membranes were boiled 30min in distilled water and then blocked with 0.5% FISH gelatin in TBST. Otherwise blocking and antibody solutions contained 5% milk. Visualisation and quantitation of western blots was carried out using an Odyssey infrared scanner (LI-COR Biosciences, Lincoln, NE).

Antibodies, Plasmids and Reagents - Antibody sources were as follows: anti-USP21 (Sigma, HPA028397), anti-Gli1 (clone L42B10, Biolabs, 2643S), anti-CUL3 (Bethyl, A301-109A), anti-ubiquitin (clone P4G7, Covance, MMS-258R), anti-HA (clone 16B12, Covance, MMS-101P), Polyclonal anti-Flag (Sigma, F7425), Monoclonal anti-Flag (clone M2, Sigma, F3165), anti-GFP and anti-RFP (sheep and rabbit respectively, gift of Ian Prior), anti-beta-actin (Abcam, ab6276), anti-Pericentrin (Abcam, ab4448), anti-PKAC (BD BioSciences, 610980).HDAC1 antibody was obtained from Santa-Cruz (sc-6298), and anti-Myc from Millipore (clone 4A6, 05-724). MLN4924 was obtained from Millenium Pharmaceuticals.

Cloning primer sequences used in this work are shown in Supplementary Table 3. pCXN2-Flag-KCTD6, pCMV-3HA-Gli1 (G933D), pGLB3B-12Gli-Luc and pRL-Renilla-TK plasmids were previously described (Canettieri et al., 2010; De Smaele et al., 2011). KCTD6 was amplified from a liver cDNA library, inserted into pCR4-TOPO (Invitrogen), and subcloned into pCMV-Tag2B-Flag vector. KCTD6 [114-237] was amplified from pCR4-TOPO-KCTD6, inserted into pET151 vector and subcloned into pCMV-Tag2B-Flag vector. pGFP-GW, pGFP-GW-USP21, pGFP-GW-USP21CS, pGFP-C1-USP21[1-174], pGFP-C1-USP21[1-210], pGFP-C1-USP21[Δ1-47], pGFP-C1-USP21[Δ1-121] and pGFP-USP21[Δ1-184] plasmids were previously described (Urbe et al., 2012). pCDNA4-CUL3-[1-250]-Flag and pCDNA4-CUL3-H2x5 H5x2 [L52A, E55A, Y58A, R59A, Y62A, Y125A and R128A] plasmids were kindly provided by Michael Rape (University of California, Berkeley, USA). Myc, Myc-USP21 and Myc-USP21CS plasmids were previously described (Urbe et al., 2012). pCXN2-Flag-KCTD11, pCXN2-Flag-KCTD21 and pCDNA-Flag-Gli1 have previously been used in (Canettieri et al., 2010; De Smaele et al., 2011). Murine Gli2 cDNA was kindly

provided by Hiroshi Sasaki and sub-cloned by means of BamHI-NotI restriction digestion in a pCDNA3-vector engineered to contain an in-frame 5' flag sequence. CRISPR plasmids expressing Cas9-GFP from a CMV promoter and selected gRNAs from a U6 promoter were kindly provided by Horizon Discoveries, Ltd (Cambridge, UK). The gRNAs used were designed to target the second exon of USP21 gene, encompassing the start codon (Supplementary Table 4). PKI-Cherry plasmid was kindly provided by Oliver Rocks (Max Delbrück Center for Molecular Medicine, Berlin). Smoothened Agonist (SAG, CAS 364590-63-6) was purchased from Calbiochem.

Dephosphorylation Assay - Cells were lysed in NP40-lysis buffer supplemented with 10mM NEM, mammalian protease and phosphatase inhibitors. Lysates (500µg) were incubated with Protein G-beads and HA antibody for 1h at 4°C. Beads were washed 3 times with YP-IP buffer, and once with 1X CutSmart buffer (NEB). Beads were resuspended in 40µl CutSmart buffer and 3µl Calf Intestinal Alkaline Phosphatase, (CIP, NEB), incubated for 1h at 30°C and the reaction was stopped by adding 5mM of EDTA and subsequent incubation at 65°C for 30min. Equivalent reaction volumes were loaded on a gel and evaluated by western-blot.

Modelling the C-terminal domain of KCTD6 - Possible distant homology of the C-terminal domain of KCTD6 with known domains or structures was assessed using HHpred (Soding, 2005) and the META-server (Bujnicki et al., 2001). *Ab initio* modelling was done with ROSETTA (Rohl et al., 2004) or QUARK (Xu and Zhang, 2012). QUARK returns 10 ranked fold predictions derived from clustering of *ab initio* models. Likewise, ten candidate structure predictions were derived from 1000 *ab initio* models using the clustering algorithm of the ROSETTA suite. Structural similarity of predictions to known folds was assessed with DALI (Holm and Sander, 1993) and the classifications of proteins of interest in the SCOP database (Andreeva et al., 2008) consulted.

Immunofluorescence - Cells on coverslips were rinsed once with PBS, fixed at -20°C with Methanol, blocked in 10% goat serum, and incubated with primary and secondary antibodies in 5% goat serum (1h each), all in PBS. Secondary antibody was conjugated to Alexa Fluor 594 or 355. Immunofluorescence images were taken using a 3i Spinning Disk microscope (63x Oil objective) and a digital camera

(Hamatsu, CMOS). The images were then processed using SlideBook software and Photoshop CS4 Version 11.0 (Adobe). Pearson's correlation coefficients were calculated using Coloc2 Plugin on Fiji.

Statistics - P values are indicated as *P,0.05, **P,0.01 and ***P,0.001 and derived either by two tailed paired t-test or, for multiple comparison analysis, by one-way ANOVA and Dunnett's post-hoc test using GraphPad Prism6.

ACKNOWLEDGMENTS

The authors thank Oliver Rocks, Michael Rape, and Horizon Discovery Ltd for generously providing plasmids and antibodies; Rebecca Eccles and Oliver Rocks for providing comments to the manuscript.

COMPETING INTERESTS

No competing interests declared.

AUTHOR CONTRIBUTIONS

CH, SU and MJC designed and interpreted the experiments, with input from EDS in some experiments. CH was responsible for the execution of the experiments with assistance by DC for experiments shown in Figure 4. CH, SU and MJC were responsible for drafting and revising the manuscript. EDS provided key reagents and was involved in revising the manuscript. DJR was responsible for the bioinformatics analysis and ab initio modeling experiments described in Figure 3. EB contributed to critical experiments for the resubmission of the manuscript.

FUNDING

This work was supported by a Wellcome Trust grant 090560/Z/09/Z.

REFERENCES:

Amakye, D., Jagani, Z. and Dorsch, M. (2013). Unraveling the therapeutic potential of the Hedgehog pathway in cancer. *Nat Med* **19**, 1410-22.

Andreeva, A., Howorth, D., Chandonia, J. M., Brenner, S. E., Hubbard, T. J., Chothia, C. and Murzin, A. G. (2008). Data growth and its impact on the SCOP database: new developments. *Nucleic Acids Res* **36**, D419-25.

Arquint, C., Gabryjonczyk, A. M. and Nigg, E. A. (2014). Centrosomes as signalling centres. *Philos Trans R Soc Lond B Biol Sci* **369**.

Bennett, E. J., Rush, J., Gygi, S. P. and Harper, J. W. (2010). Dynamics of cullin-RING ubiquitin ligase network revealed by systematic quantitative proteomics. *Cell* **143**, 951-65.

Briscoe, J. and Therond, P. P. (2013). The mechanisms of Hedgehog signalling and its roles in development and disease. *Nat Rev Mol Cell Biol* **14**, 416-29.

Bujnicki, J. M., Elofsson, A., Fischer, D. and Rychlewski, L. (2001). Structure prediction meta server. *Bioinformatics* **17**, 750-1.

Canettieri, G., Di Marcotullio, L., Greco, A., Coni, S., Antonucci, L., Infante, P., Pietrosanti, L., De Smaele, E., Ferretti, E., Miele, E. et al. (2010). Histone deacetylase and Cullin3-REN(KCTD11) ubiquitin ligase interplay regulates Hedgehog signalling through Gli acetylation. *Nat Cell Biol* **12**, 132-42.

Chen, J. K., Taipale, J., Young, K. E., Maiti, T. and Beachy, P. A. (2002). Small molecule modulation of Smoothened activity. *Proc Natl Acad Sci U S A* **99**, 14071-6.

Chen, Y. and Jiang, J. (2013). Decoding the phosphorylation code in Hedgehog signal transduction. *Cell Res* **23**, 186-200.

Clague, M. J., Barsukov, I., Coulson, J. M., Liu, H., Rigden, D. J. and Urbe, S. (2013). Deubiquitylases from genes to organism. *Physiol Rev* **93**, 1289-315.

Clague, M. J., Coulson, J. M. and Urbe, S. (2012a). Cellular functions of the DUBs. *J Cell Sci* **125**, 277-86.

Clague, M. J., Liu, H. and Urbe, S. (2012b). Governance of endocytic trafficking and signaling by reversible ubiquitylation. *Dev Cell* **23**, 457-67.

Cummins, J. M. and Vogelstein, B. (2004). HAUSP is required for p53 destabilization. *Cell Cycle* **3**, 689-92.

Dahmane, N., Lee, J., Robins, P., Heller, P. and Ruiz i Altaba, A. (1997). Activation of the transcription factor Gli1 and the Sonic hedgehog signalling pathway in skin tumours. *Nature* **389**, 876-81.

De Smaele, E., Di Marcotullio, L., Moretti, M., Pelloni, M., Occhione, M. A., Infante, P., Cucchi, D., Greco, A., Pietrosanti, L., Todorovic, J. et al. (2011). Identification and characterization of KCASH2 and KCASH3, 2 novel Cullin3 adaptors suppressing histone deacetylase and Hedgehog activity in medulloblastoma. *Neoplasia* **13**, 374-85.

Diercks, T., Ab, E., Daniels, M. A., de Jong, R. N., Besseling, R., Kaptein, R. and Folkers, G. E. (2008). Solution structure and characterization of the DNA-binding activity of the B3BP-Smr domain. *J Mol Biol* **383**, 1156-70.

Fukui, K., Kosaka, H., Kuramitsu, S. and Masui, R. (2007). Nuclease activity of the MutS homologue MutS2 from Thermus thermophilus is confined to the Smr domain. *Nucleic Acids Res* **35**, 850-60.

Gerdes, J. M., Liu, Y., Zaghloul, N. A., Leitch, C. C., Lawson, S. S., Kato, M., Beachy, P. A., Beales, P. L., DeMartino, G. N., Fisher, S. et al. (2007).

Disruption of the basal body compromises proteasomal function and perturbs intracellular Wnt response. *Nat Genet* **39**, 1350-60.

Goetz, S. C. and Anderson, K. V. (2010). The primary cilium: a signalling centre during vertebrate development. *Nat Rev Genet* **11**, 331-44.

Gonnissen, A., Isebaert, S. and Haustermans, K. (2015). Targeting the Hedgehog signaling pathway in cancer: beyond Smoothened. *Oncotarget* **6**, 13899-913.

Gosens, I., van Wijk, E., Kersten, F. F., Krieger, E., van der Zwaag, B., Marker, T., Letteboer, S. J., Dusseljee, S., Peters, T., Spierenburg, H. A. et al. (2007). MPP1 links the Usher protein network and the Crumbs protein complex in the retina. *Hum Mol Genet* **16**, 1993-2003.

Gulino, A., Di Marcotullio, L., Canettieri, G., De Smaele, E. and Screpanti, I. (2012). Hedgehog/Gli control by ubiquitination/acetylation interplay. *Vitam Horm* **88**, 211-27.

Hayes, S. D., Liu, H., Macdonald, E., Sanderson, C. M., Coulson, J. M., Clague, M. J. and Urbe, S. (2012). Direct and Indirect Control of Mitogen-activated Protein Kinase Pathway-associated Components, BRAP/IMP E3 Ubiquitin Ligase and CRAF/RAF1 Kinase, by the Deubiquitylating Enzyme USP15. *J Biol Chem* **287**, 43007-18.

Holm, L. and Sander, C. (1993). Protein structure comparison by alignment of distance matrices. *J Mol Biol* **233**, 123-38.

Hui, C. C. and Angers, S. (2011). Gli proteins in development and disease. *Annu Rev Cell Dev Biol* **27**, 513-37.

Ingham, P. W., Nakano, Y. and Seger, C. (2011). Mechanisms and functions of Hedgehog signalling across the metazoa. *Nat Rev Genet* **12**, 393-406.

Jiang, J. (2006). Regulation of Hh/Gli signaling by dual ubiquitin pathways. *Cell Cycle* **5**, 2457-63.

Kan, Z., Jaiswal, B. S., Stinson, J., Janakiraman, V., Bhatt, D., Stern, H. M., Yue, P., Haverty, P. M., Bourgon, R., Zheng, J. et al. (2010). Diverse somatic mutation patterns and pathway alterations in human cancers. *Nature* **466**, 869-73.

Keusekotten, K., Elliott, P. R., Glockner, L., Fiil, B. K., Damgaard, R. B., Kulathu, Y., Wauer, T., Hospenthal, M. K., Gyrd-Hansen, M., Krappmann, D. et al. (2013). OTULIN antagonizes LUBAC signaling by specifically hydrolyzing Met1-linked polyubiquitin. *Cell* **153**, 1312-26.

Kinzler, K. W., Bigner, S. H., Bigner, D. D., Trent, J. M., Law, M. L., O'Brien, S. J., Wong, A. J. and Vogelstein, B. (1987). Identification of an amplified, highly expressed gene in a human glioma. *Science* **236**, 70-3.

Komander, D., Clague, M. J. and Urbe, S. (2009). Breaking the chains: structure and function of the deubiquitinases. *Nat Rev Mol Cell Biol* **10**, 550-63.

Krissinel, E. and Henrick, K. (2007). Inference of macromolecular assemblies from crystalline state. *J Mol Biol* **372**, 774-97.

Lancaster, M. A., Schroth, J. and Gleeson, J. G. (2011). Subcellular spatial regulation of canonical Wnt signalling at the primary cilium. *Nat Cell Biol* **13**, 700-7.

Lange, S., Perera, S., Teh, P. and Chen, J. (2012). Obscurin and KCTD6 regulate cullin-dependent small ankyrin-1 (sAnk1.5) protein turnover. *Mol Biol Cell* **23**, 2490-504.

Li, S., Chen, Y., Shi, Q., Yue, T., Wang, B. and Jiang, J. (2012). Hedgehog-regulated ubiquitination controls smoothened trafficking and cell surface expression in Drosophila. *PLoS Biol* **10**, e1001239.

Matthews, J. M. and Sunde, M. (2002). Zinc fingers--folds for many occasions. *IUBMB Life* **54**, 351-5.

Mazza, D., Infante, P., Colicchia, V., Greco, A., Alfonsi, R., Siler, M., Antonucci, L., Po, A., De Smaele, E., Ferretti, E. et al. (2013). PCAF ubiquitin ligase activity inhibits Hedgehog/Gli1 signaling in p53-dependent response to genotoxic stress. *Cell Death Differ* **20**, 1688-97.

Niewiadomski, P., Kong, J. H., Ahrends, R., Ma, Y., Humke, E. W., Khan, S., Teruel, M. N., Novitch, B. G. and Rohatgi, R. (2014). Gli protein activity is controlled by multisite phosphorylation in vertebrate Hedgehog signaling. *Cell Rep* **6**, 168-81.

Nigg, E. A., Schafer, G., Hilz, H. and Eppenberger, H. M. (1985). Cyclic-AMP-dependent protein kinase type II is associated with the Golgi complex and with centrosomes. *Cell* **41**, 1039-51.

Nolan-Stevaux, O., Lau, J., Truitt, M. L., Chu, G. C., Hebrok, M., Fernandez-Zapico, M. E. and Hanahan, D. (2009). GLI1 is regulated through Smoothened-independent mechanisms in neoplastic pancreatic ducts and mediates PDAC cell survival and transformation. *Genes Dev* **23**, 24-36.

Nusslein-Volhard, C. and Wieschaus, E. (1980). Mutations affecting segment number and polarity in Drosophila. *Nature* **287**, 795-801.

Okuda, H., Ohdan, H., Nakayama, M., Koseki, H., Nakagawa, T. and Ito, T. (2013). The USP21 short variant (USP21SV) lacking NES, located mostly in the nucleus in vivo, activates transcription by deubiquitylating ubH2A in vitro. *PLoS ONE* **8**, e79813.

Rohl, C. A., Strauss, C. E., Misura, K. M. and Baker, D. (2004). Protein structure prediction using Rosetta. *Methods Enzymol* **383**, 66-93.

Schulein-Volk, C., Wolf, E., Zhu, J., Xu, W., Taranets, L., Hellmann, A., Janicke, L. A., Diefenbacher, M. E., Behrens, A., Eilers, M. et al. (2014). Dual regulation of Fbw7 function and oncogenic transformation by Usp28. *Cell Rep* **9**, 1099-109.

Scott, J. D., Fischer, E. H., Demaille, J. G. and Krebs, E. G. (1985). Identification of an inhibitory region of the heat-stable protein inhibitor of the cAMP-dependent protein kinase. *Proc Natl Acad Sci U S A* **82**, 4379-83.

Sheng, T., Chi, S., Zhang, X. and Xie, J. (2006). Regulation of Gli1 localization by the cAMP/protein kinase A signaling axis through a site near the nuclear localization signal. *J Biol Chem* **281**, 9-12.

Shi, R., Proteau, A., Villarroya, M., Moukadiri, I., Zhang, L., Trempe, J. F., Matte, A., Armengod, M. E. and Cygler, M. (2010). Structural basis for Fe-S cluster assembly and tRNA thiolation mediated by IscS protein-protein interactions. *PLoS Biol* **8**, e1000354.

Smaldone, G., Pirone, L., Balasco, N., Di Gaetano, S., Pedone, E. M. and Vitagliano, L. (2015). Cullin 3 Recognition Is Not a Universal Property among KCTD Proteins. *PLoS ONE* **10**, e0126808.

Soding, J. (2005). Protein homology detection by HMM-HMM comparison. *Bioinformatics* **21**, 951-60.

Sowa, M. E., Bennett, E. J., Gygi, S. P. and Harper, J. W. (2009). Defining the human deubiquitinating enzyme interaction landscape. *Cell* **138**, 389-403.

Stogios, P. J., Downs, G. S., Jauhal, J. J., Nandra, S. K. and Prive, G. G. (2005). Sequence and structural analysis of BTB domain proteins. *Genome Biol* **6**, R82.

Takebe, N., Miele, L., Harris, P. J., Jeong, W., Bando, H., Kahn, M., Yang, S. X. and Ivy, S. P. (2015). Targeting Notch, Hedgehog, and Wnt pathways in cancer stem cells: clinical update. *Nat Rev Clin Oncol* **12**, 445-64.

Tariki, M., Dhanyamraju, P. K., Fendrich, V., Borggrefe, T., Feldmann, G. and Lauth, M. (2014). The Yes-associated protein controls the cell density regulation of Hedgehog signaling. *Oncogenesis* **3**, e112.

Terrin, A., Monterisi, S., Stangherlin, A., Zoccarato, A., Koschinski, A., Surdo, N. C., Mongillo, M., Sawa, A., Jordanides, N. E., Mountford, J. C. et al. (2012). PKA and PDE4D3 anchoring to AKAP9 provides distinct regulation of cAMP signals at the centrosome. *J Cell Biol* **198**, 607-21.

Tuson, M., He, M. and Anderson, K. V. (2011). Protein kinase A acts at the basal body of the primary cilium to prevent Gli2 activation and ventralization of the mouse neural tube. *Development* **138**, 4921-30.

Urbe, S., Liu, H., Hayes, S. D., Heride, C., Rigden, D. J. and Clague, M. J. (2012). Systematic survey of deubiquitinase localisation identifies USP21 as a regulator of centrosome and microtubule associated functions. *Mol Biol Cell* **23**, 1095-1103.

Villeneuve, N. F., Tian, W., Wu, T., Sun, Z., Lau, A., Chapman, E., Fang, D. and Zhang, D. D. (2013). USP15 negatively regulates Nrf2 through deubiquitination of Keap1. *Mol Cell* **51**, 68-79.

Wang, W., Lundin, V. F., Millan, I., Zeng, A., Chen, X., Yang, J., Allen, E., Chen, N., Bach, G., Hsu, A. et al. (2012a). Nemitin, a novel Map8/Map1s interacting protein with Wd40 repeats. *PLoS ONE* **7**, e33094.

Wang, Y., Ding, Q., Yen, C. J., Xia, W., Izzo, J. G., Lang, J. Y., Li, C. W., Hsu, J. L., Miller, S. A., Wang, X. et al. (2012b). The crosstalk of mTOR/S6K1 and Hedgehog pathways. *Cancer Cell* **21**, 374-87.

Xia, R., Jia, H., Fan, J., Liu, Y. and Jia, J. (2012). USP8 Promotes Smoothened Signaling by Preventing Its Ubiquitination and Changing Its Subcellular Localization. *PLoS Biol* **10**, e1001238.

Xu, D. and Zhang, Y. (2012). Ab initio protein structure assembly using continuous structure fragments and optimized knowledge-based force field. *Proteins* **80**, 1715-35.

Ye, Y., Akutsu, M., Reyes-Turcu, F., Enchev, R. I., Wilkinson, K. D. and Komander, D. (2011). Polyubiquitin binding and cross-reactivity in the USP domain deubiquitinase USP21. *EMBO Rep*.

Zhang, H., Xu, Q., Lu, M., Xu, X., Wang, Y., Wang, L., Zhao, Y. and Hua, Y. (2014). Structural and functional studies of MutS2 from Deinococcus radiodurans. *DNA Repair (Amst)* **21**, 111-9.

Zhou, Z., Yao, X., Li, S., Xiong, Y., Dong, X., Zhao, Y., Jiang, J. and Zhang, Q. (2015). Deubiquitination of Ci/Gli by Usp7/HAUSP Regulates Hedgehog Signaling. *Dev Cell* **34**, 58-72.

FIGURE LEGENDS

Figure 1: USP21 interacts with KCTD6, a component of the BTB-CUL3-Rbx1 Ubiquitin E3 ligase complex

(A) A Y2H screen of a normalised human cDNA library using USP21 [Δ1-47] as a bait identifies the CUL3-substrate-adapter protein KCTD6 [1-187]. USP, ubiquitin specific protease; BTB, Broad-Complex, Tramtrack and Bric a brac. A Smr-like domain (SmrL) was identified by *ab initio* modeling (see Figure 3).

(B) Validation of the interaction of USP21 with KCTD6 in human cells. HEK293T cells were transfected with Flag-KCTD6 and either GFP, GFP-USP21 or GFP-USP21CS. Lysates were subjected to immunoprecipitation with GFP or Flag antibodies.

(C) Inactive USP21 co-precipitates ubiquitylated KCTD6. Lysates were used for immunoprecipitation with anti-GFP antibody. Interacting proteins were analysed by western blot with anti-Flag and anti-Ubiquitin (P4G7) antibodies. Exp: exposure

(B, C) Arrowheads indicate mono- (<) and di-(<<)ubiquitylated species of KCTD6. Arrow indicates unmodified KCTD6.

(D) The higher molecular weight form of USP21-C221S (arrow) corresponds to a mono-ubiquitylated species. Lysates from the experiment shown in C were subjected to immune-precipitation with anti-GFP antibodies and probed in parallel with anti-Ubiquitin or anti-GFP antibodies.

Figure 2: Indirect interaction of USP21 with Cullin 3

(A) Diagram of the featured CUL3 constructs: Full-length CUL3, a BTB-domain binding mutant (CUL3m) and a dominant negative C-terminal truncation mutant (CUL3 [1-250]). Asterisks indicate point mutations.

(B) USP21 interacts with CUL3 in HEK293T cells. HEK293T cells were transfected as indicated and lysates subjected to immunoprecipitation with GFP and Flag antibodies respectively. Asterisk indicates a higher molecular weight form of Flag-CUL3.

(C,D) HEK293T cells were cotransfected with USP21 and with either CUL3m (C) or with CUL3 [1-250] (D). Protein lysates were subjected to immunoprecipitation with anti-GFP or anti-Flag. The interacting proteins were analysed by western blot with anti-GFP and either anti-CUL3 or anti-Flag.

Figure 3: Mapping the interaction between USP21 and KCTD6-CUL3 E3 Ligase complex

(A) USP21 interacts with KCTD6 [114-237]. HEK293T cells were transfected with Full-length (FL) or truncated KCTD6, GFP or GFP-USP21, and IPs were performed and analysed as indicated.

(B) The overall fold similarity between the favoured QUARK *ab initio* model of the KCTD6 Smr-like domain (SmrL [109-213]) and the C-terminal Smr domain of human NEDD4-binding protein 2 (PDB code 2vkc;1400 Diercks,T. 2008). Each is coloured in a spectrum from blue (N-terminus) to red (C-terminus). A broken line indicates the boundary between the functionally dispensable C-terminal region [188-213] and the remainder.

(C,D) HEK293T cells transfected with Flag-KCTD6 (C) or Flag-CUL3 (D) and GFP-tagged USP21 fragments were lysed in RIPA buffer. Protein lysates were used for IP with GFP antibody. Asterisk indicates a mono-ubiquitylated form of Flag-KCTD6.

(E) Diagram summarising the interactions between USP21 and KCTD6 and CUL3, components of the BTB-Cullin3-Rbx1 E3 Ligase complex. USP21[Δ1-184] is both necessary and sufficient for the interaction with KCTD6 [114-187]. Cullins share a homologous C-terminus that interacts with the Ring-finger protein Rbx1.

Figure 4: USP21 modulates Hedgehog signaling and Gli1 transcriptional activity

(A) NIH3T3 cells were treated with USP21-targeting siRNA oligos (#10, 11, 12) or a non-targeting control (NT3), serum starved and then incubated with SAG (100nM) for 4h prior to mRNA extraction. USP21 and Gli1 mRNA levels were measured by qRT-PCR and normalised to RNA Pol2 (n=3 independent experiments, ±SD).

(B) HEK293T cells were treated with USP21-targeting siRNA-oligos (#5, #6) or non-targeting control oligo (NT3), or treated with transfection reagent alone (Mock). 24 hours before lysis, cells were transfected with Gli-responsive firefly luciferase and Renilla luciferase reporters (pGLB3B-12Gli-Luc and pRL-Renilla-TK) as well as with a Gli1 expression construct (HA-Gli1). Efficiency of the knockdown was assessed by western-blotting. (n=2, bar=range)

(C) HEK293T cells were transfected with Gli-responsive firefly luciferase, Renilla luciferase reporters, 3HA-Gli1 and indicated amounts of GFP, GFP-USP21 or GFP-USP21CS plasmids. GFP-protein expression was assessed by western-blotting.

(GFP: n=5; USP21/CS: n=6, ±SD, one-way ANOVA and Dunnett's test)

Figure 5: USP21 regulates Gli1 expression levels

(A) USP21 knockout results in a decrease in endogenous Gli1 protein. HEK293T cells were transfected with plasmids encoding both Cas9-GFP and one of 5 independent CRISPR gRNAs targeting USP21. Cells were lysed in RIPA lysis buffer 72h after transfection. Protein lysates were assessed by western-blot (representative experiment). Arrow indicates the major USP21 isoform (63kDa) (Okuda et al., 2013). The scatter plot illustrates the close correlation between USP21 and Gli1 protein levels across conditions. Pink and blue dots indicate Mock and USP21 gRNA respectively.

(B) USP21 overexpression increases Gli1 protein levels. HEK293T cells were cotransfected with indicated plasmids. Protein lysates were evaluated by western-blot.

(C) USP21 interacts with Gli1. Lysates shown in (B) were subjected to immunoprecipitation with HA antibody.

(D) KCTD6 counteracts USP21 dependent Gli1 stabilisation. HEK293T cells were transfected with HA-Gli1 and GFP-USP21 and increasing amount of Flag-KCTD6. Protein lysates were assessed by western-blot. (n=3; ±SD; one-way ANOVA and Dunnett's test).

Figure 6: USP21 recruits Gli1 to the centrosome and promotes its phosphorylation by PKA.

(A) HEK293T were transfected with indicated plasmids for 24h. Protein expression was assessed by western-blotting with HA and GFP antibodies. Graph shows the quantitation of the upper form of HA-Gli1 (n=3, ±SEM, one-way ANOVA and Dunnett's test).

(B) HEK293T were lysed 24h after transfection with the indicated plasmids, immunoprecipitated HA-Gli1 was incubated with Alkaline Phosphatase (CIP) at 30°C for 1h. Red arrowheads (<) indicate the upper phosphorylated band.

(C) HEK293T were transfected with HA-Gli1, GFP or GFP-USP21 and increasing amounts (µg) of PKI-Cherry or RFP control. Cells were lysed 24h after transfection. Protein levels were assessed by western-blotting with HA and RFP antibodies and membranes were reprobed with anti-GFP.

(D) USP21 colocalises with the catalytic subunit of PKA (PKAC) at centrosomes. U2OS cells were transfected with GFP-USP21 or GFP alone as a control. After MeOH fixation, cells were stained with anti-PKAC (red) and anti-Pericentrin (blue) antibodies. Images were captured with a 3i Spinning Disk confocal microscope (63x objective).

(E) USP21 and Gli1 colocalize at the centrosome. U2OS cells were co-transfected with HA-Gli1 and GFP-USP21 or GFP-USP21CS. After MeOH fixation, cells were stained with Gli1 (red) and Pericentrin (blue) antibodies. Images were captured with a 3i Spinning Disk (63x objective). Pearson correlation coefficients for Gli1 or GFP colocalisation with Pericentrin were calculated on ≥33 cells per condition. Scale bar = 10μm.

(F) Working model illustrating the dual role of USP21 in regulating Gli1. USP21 recruits Gli1 at the centrosome and thereby promotes consequential phosphorylation by PKA. PKA may act as a priming kinase for further phosphorylation and ubiquitylation events. Wild-type but not catalytically inactive USP21 is able to stabilise the labile pool of phosphorylated Gli1.

Clone	Protein Name	Gene ID	Region Interacting v USP21[Δ 1-47] (aa)
#1	BTB/POZ domain-containing protein KCTD6	200845	1-187
#2	WD repeat containing protein 47 WDR47	22911	685-927
#3	Spectrin repeat containing, nuclear envelope 1 SYNE1	23345	2940-3140
#4	Zinc finger protein 350 ZNF350	59348	292-530
#5	Zinc finger protein 350 ZNF350	59348	291-415
#6	Membrane protein, palmitoylated 1, 55kDa MPP1	4354	318-466
#7	Ankyrin repeat domain containing protein 32 ANKRD32	84250	802-1058

Table 1: Identification of potential interacting proteins of USP21 by Yeast-two-Hybrid using a Human normalised library. Seven clones encoding six new candidate interactors for USP21 were isolated from a Human normalized prey cDNA library using an USP21-bait construct encoding aa 48-565. Abbreviations: aa, amino-acids

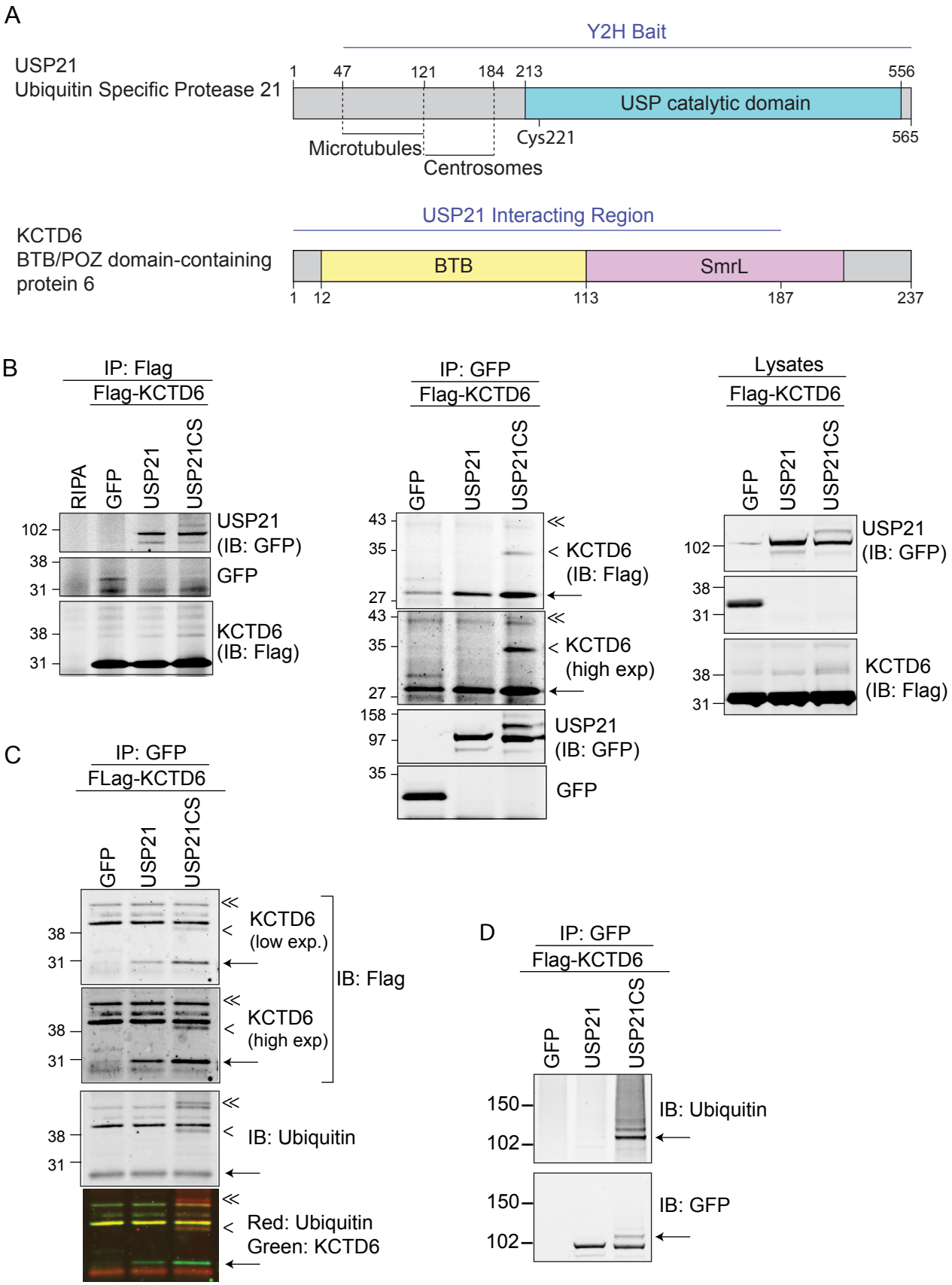

Heride et al., Figure 1

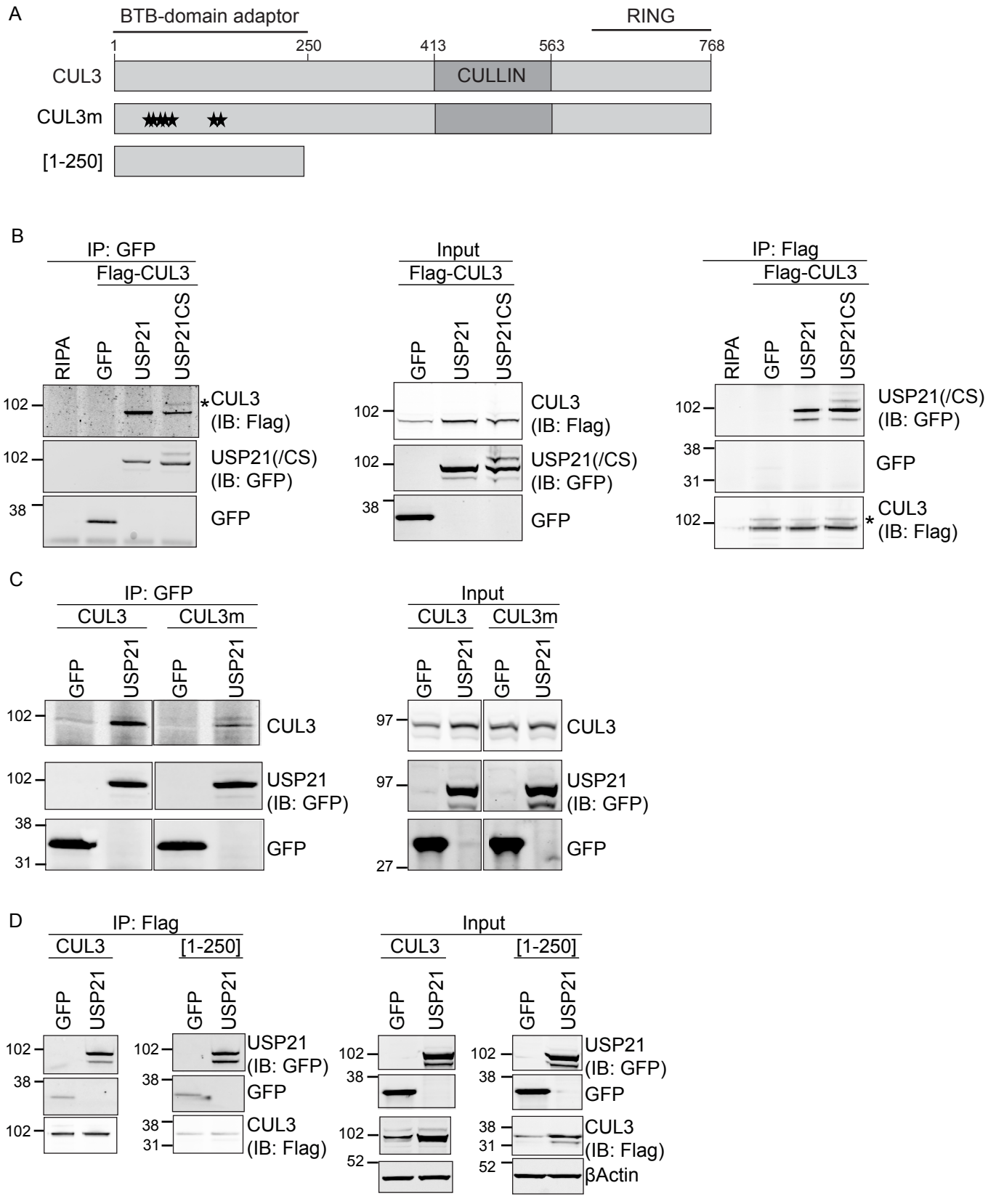

Heride et al., Figure 2

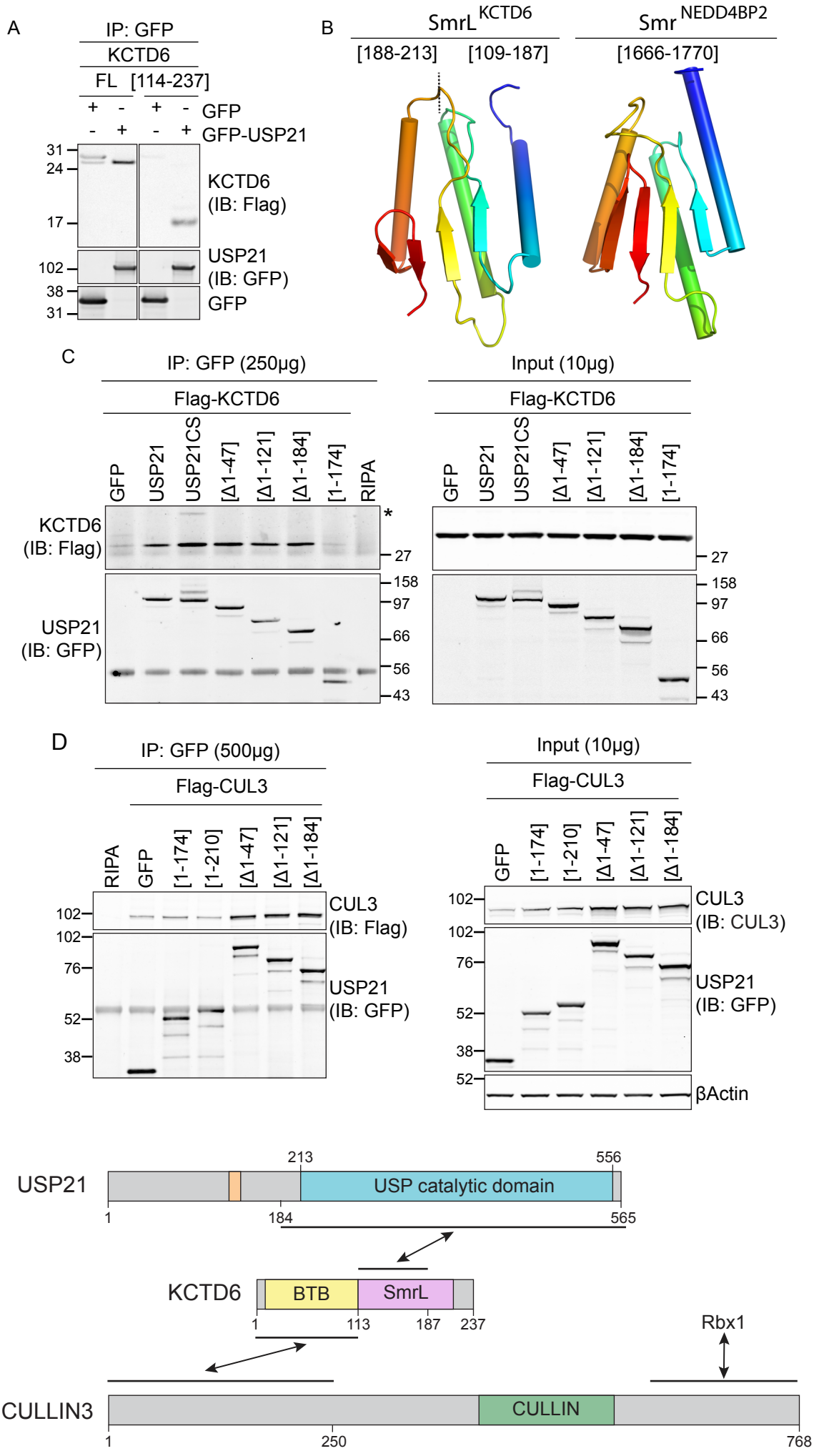

Heride et al., Figure 3

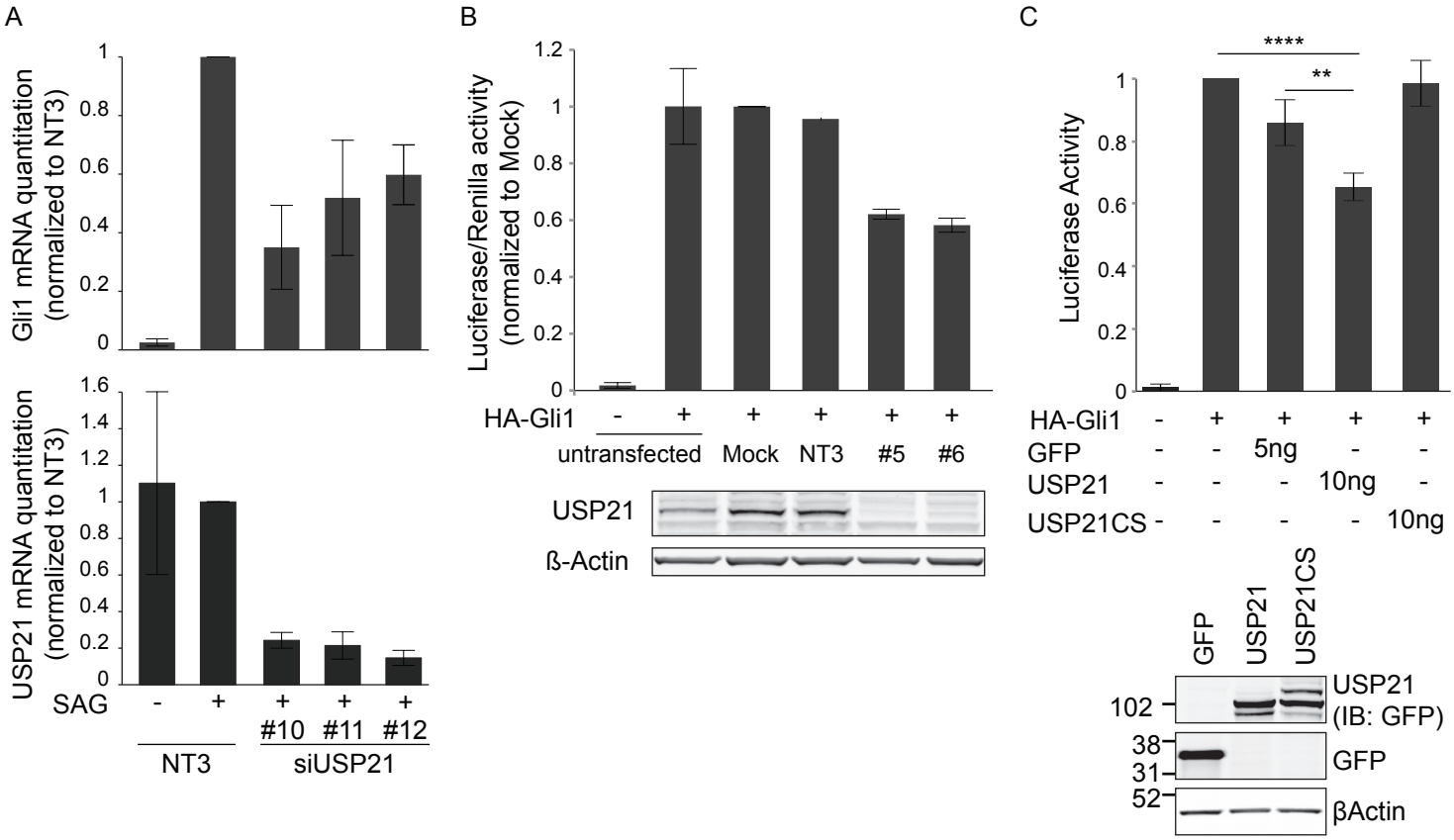

Heride et al., Figure 4

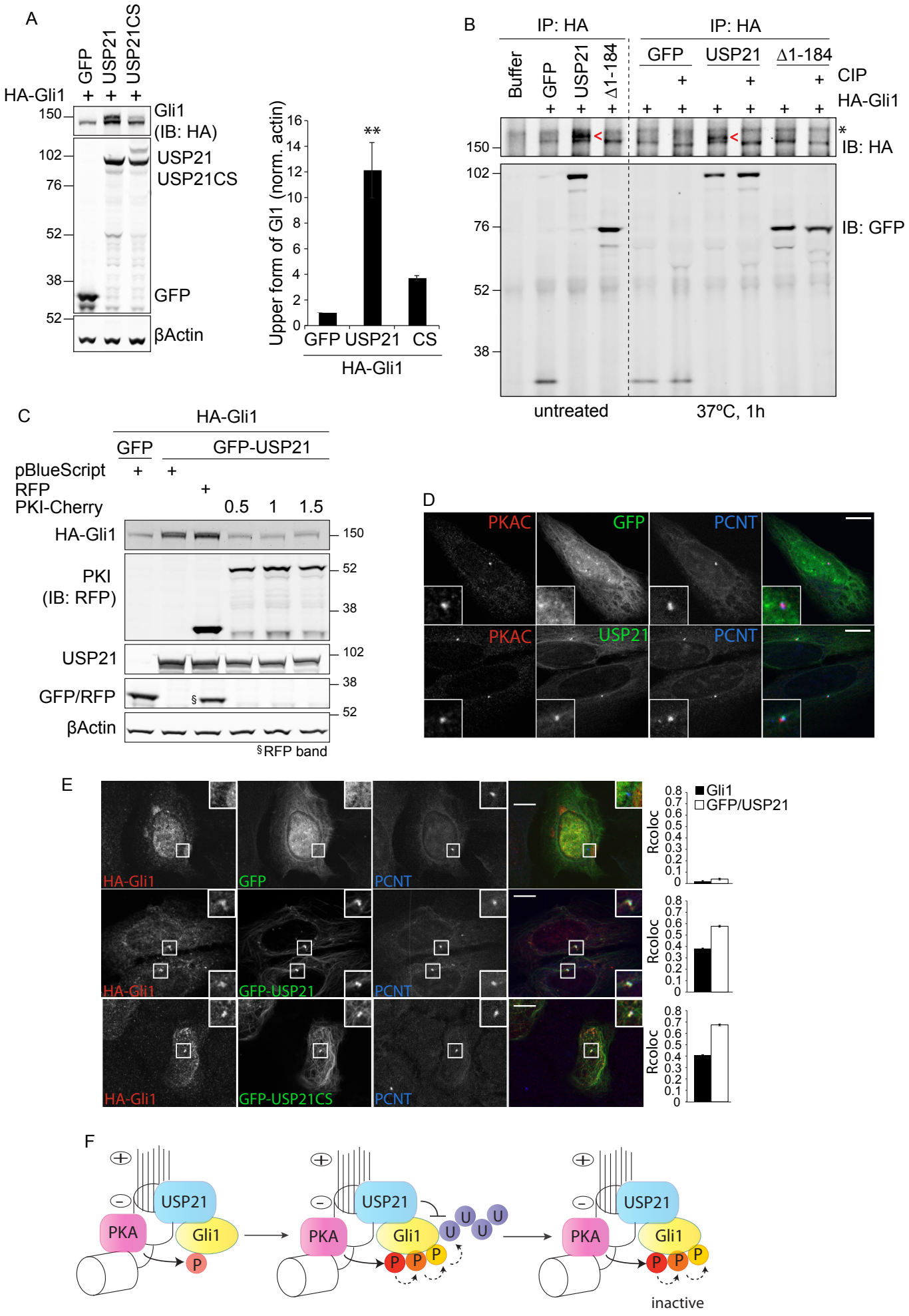

Heride et al., Figure 6

SUPPLEMENTAL Tables:

Supplementary Table 1: siRNA oligos (DHARMACON Thermoscientific)			
siRNA names	Gene ID	Catalog number	Sequence
Hs USP21 siRNA#5	27005	J-006071-05	CCACCCACUUUGAGACGUA
Hs USP21 siRNA#6	27005	J-006071-06	GAUCCAAGCUACCAUUUGC
Hs USP21 siRNA#7	27005	J-006071-07	CGAGAGCCACCUGUUAAUA
Hs USP21 siRNA#8	27005	J-006071-08	CUUCGGGACUUCUGUCUGA
Hs Gli1 siRNA (On Target Plus Pool)	2735	L-003896-00	GCAAAUAGGGCUUCACAUA AGGCUCAGCUUGUGUGUAA GGACGAGGGACCUUGCAUU CAGCUAGAGUCCAGAGGUU
Mm USP21 siRNA#10	30941	J-063216-10	ACUUAAUGUGGAAGCGCUA
Mm USP21 siRNA#11	30941	J-063216-11	UACAAUGACUCCCGCGUUU
Mm USP21 siRNA#12	30941	J-063216-12	CUUCCUGAAUGCCGUGCUA
NT1		D-001810-01	UGGUUUACAUGUCGACUAA
NT3		D-001810-03	UGGUUUACAUGUUUUCUGA

Supplementary Table 2: QPCR Primers

Target	Primer Name	Primer Sequence
Gli1	Gli1_Mm_Forward	CCA GCA GCT GCA CTG AAG GAT C
	Gli1_Mm_Reverse	CCA GCT CTG ACT TCA GCT GG
USP21	USP21_Mm_Forward	CTG ATG ACA AGA TGG CTC ACC AC
	USP21_Mm_Reverse	CCA ATC ACA TCT GCA AAG GCT TCT G
POL2	POL2_Mm_Forward	CCGGAAGCTTACCATGGAAC
	POL2_Mm_Reverse	TGTCTGTCTGAGGTAAGTGC

Supplementary Table 3: Cloning Primers

Target	Primer Name	Primer Sequence
KCTD6	KCTD6_lib-Forward	CT GGG CTC TTG AAG ACG C
	KCTD6_lib-Reverse	GGA GAG TCT TTC CAG GAA CC
	KCTD6_aa114-Forward	CATATGatggatactttgaagaagttgtgg
	KCTD6_aa237_Reverse	GTCGACtcagtcgtctgtcttccgggctagcctacag
MPP1	MPP1_lib- Forward	GTCTTGCGTTCCAGTGTTCC
	MPP1_ lib-Reverse	AGTGGGTTCCCCCATTCTAC

Supplementary Table 4: USP21 CRISPR gRNA

gRNA name	Guide id	Sequence
USP21gRNA#2	47002	GCATTGTGGACACCACAGGC
USP21gRNA#3	47003	CAGGCGGTGCTCAGAGGCCT
USP21gRNA#4	47004	TAACAGGTGGCTCTCGGGTA
USP21gRNA#5	47005	GGTAGCTTGGATCCCACTCG
USP21gRNA#6	47006	CTCCTTGCTGCGGGCCCTGG

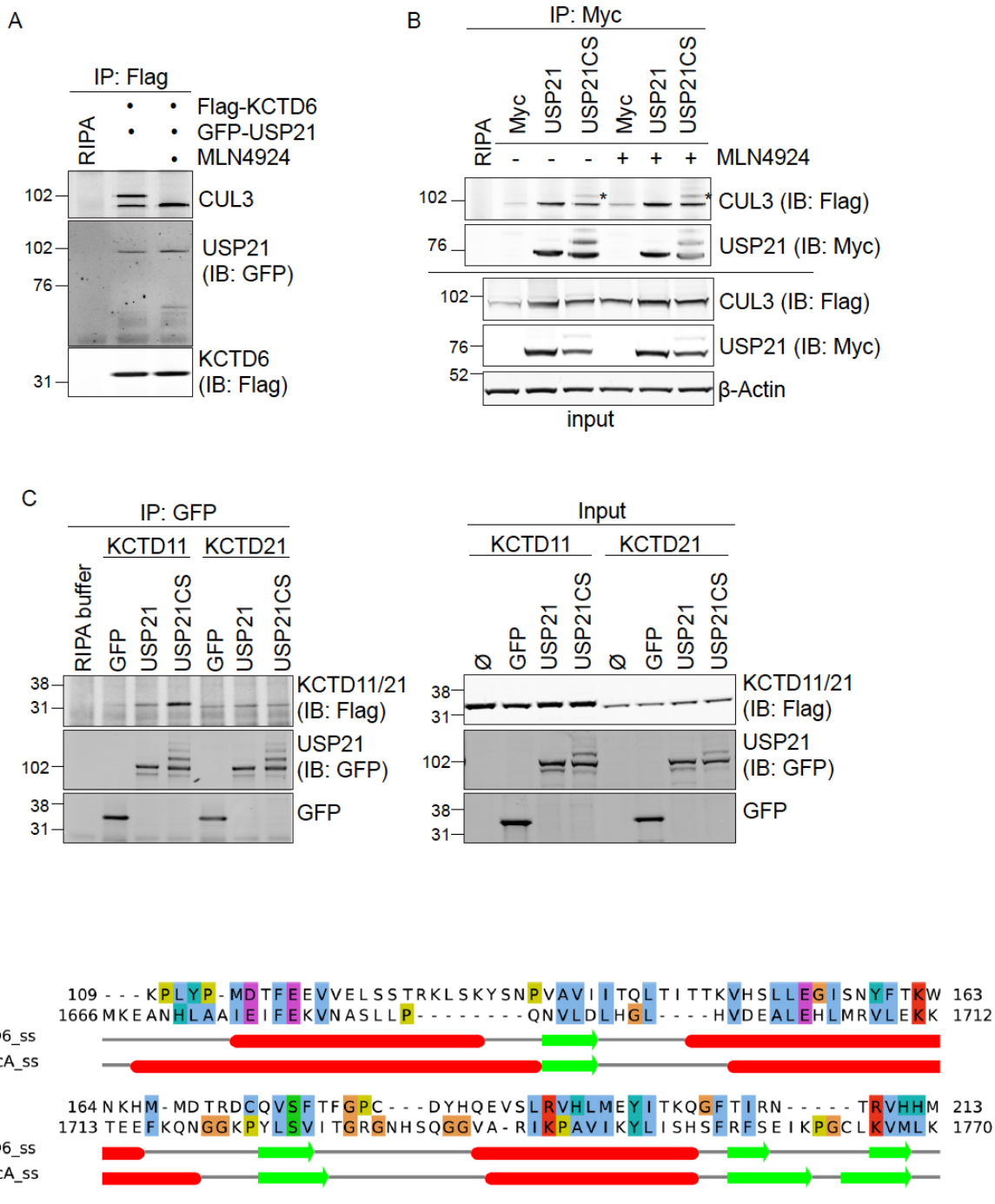

Supplementary Figure 1:
(A) The substrate adaptor KCTD6 interacts with neddylated and de-neddylated CUL3. HEK293T were transfected with GFP-USP21 and Flag-KCTD6 and then incubated with 1μM of MLN4924 or DMSO for 4h. Protein lysates were used for IP with Flag antibody.
(B) Interaction of USP21 with CUL3 is not affected by MLN4924 treatment. HEK293T were transfected with the indicated plasmids for 24h and then incubated with 1μM MLN4924 or DMSO for 4h before being lysed and subjected to IP. Asterisks indicate higher molecular weight forms of CUL3.

(C) USP21 interacts with KCTD11 but not KCTD21. HEK293T cells were transfected with Flag-KCTD11 or Flag-KCTD21 together with GFP, GFP-USP21 or GFP-USP21-C221S (CS). Protein lysates were subjected to immunoprecipitation with GFP antibody.
(D) Structure alignment of favoured QUARK *ab initio* model of KCTD6 [109-213] and the C-terminal Smr domain of human NEDD4-binding protein 2 (PDB code 2vkc;1400 Diercks,T. 2008). The alignment results from a DALI database search and achieved a Z-score of 7.1. Jalview was used to display the alignment and to annotate regular secondary structure elements seen in model and NMR structure (red α-helices; green β-strands) (Waterhouse, A. M. et al., 2009 Bioinformatics 25, 1189-91).

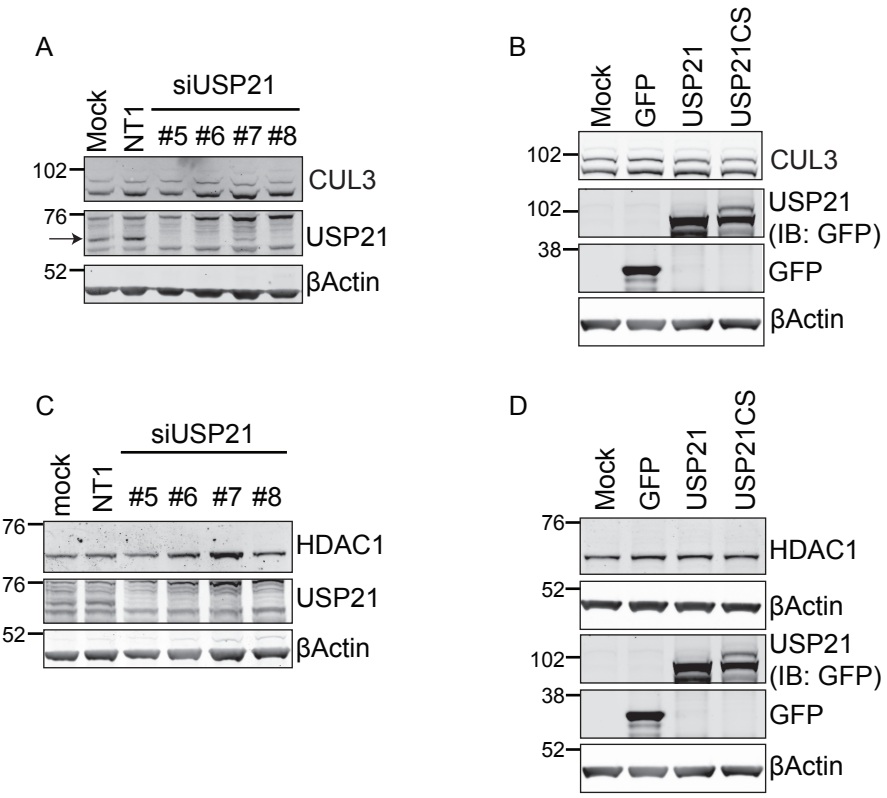

Supplementary Figure 2:
(A,B) CUL3 protein level and neddylation are not regulated by USP21. U2OS cells were transfected either with USP21 siRNA oligos (A) or with GFP, GFP-USP21 or GFP-USP21CS (B). CUL3 protein levels were assessed by western-blotting with a CUL3 specific antibody.
(C,D) USP21 does not regulate HDAC1 protein level. U2OS cells were transfected either with USP21 siRNA oligos (C) or with GFP-USP21CS (D). Endogenous HDAC1 was assessed by western-blot.

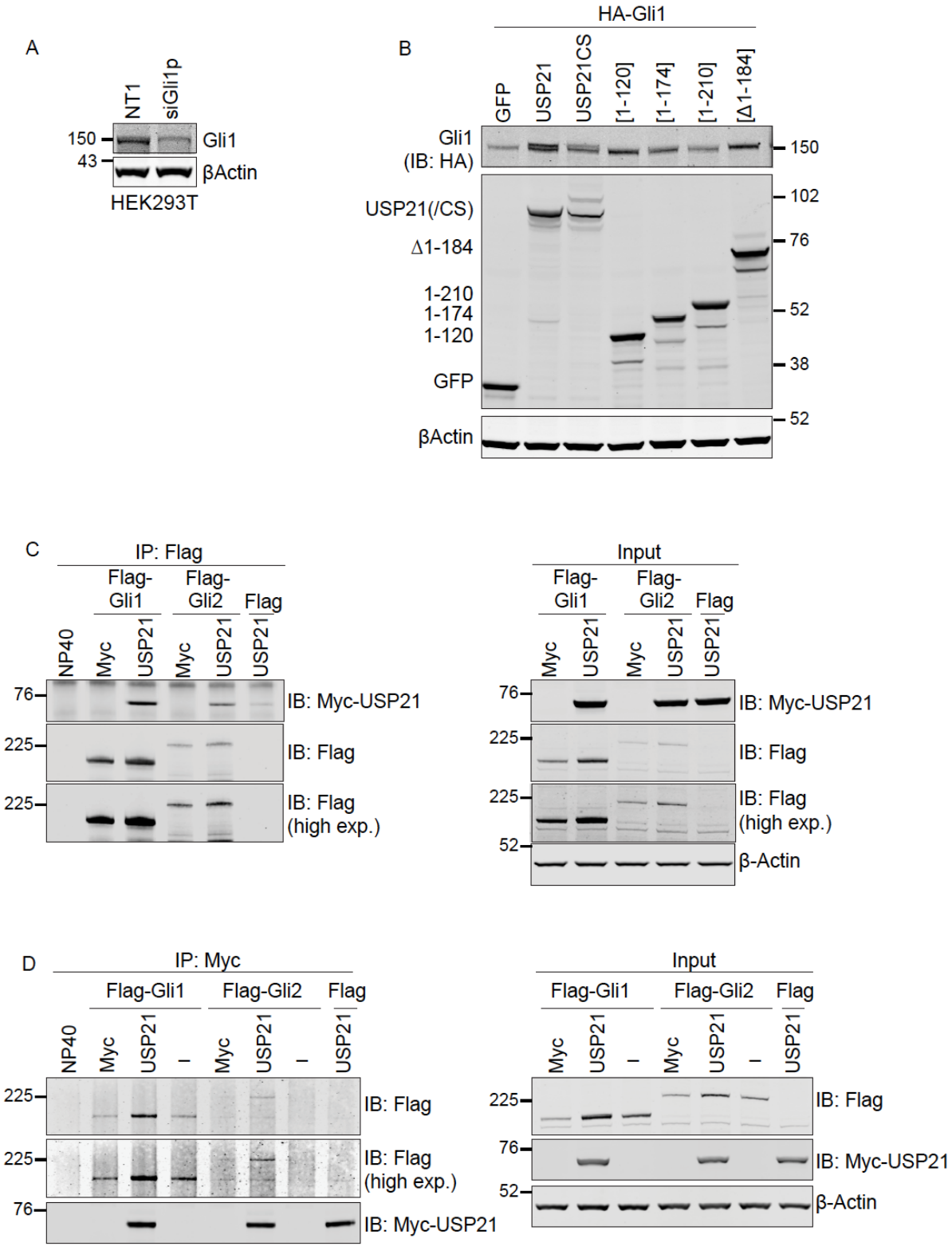

Supplementary Figure 3: USP21 promotes Gli1 stabilisation and interacts with Gli1 and Gli2.

(A) HEK293T cells express low levels of endogenous Gli1. HEK293T cells were treated for 96 hours with siRNA targeting Gli1 (siGli1p, On Target Plus pool), lysed and proteins were subjected to western blot analysis.

(B) USP21 overexpression induces Gli1 stabilisation. HEK293T cells were cotransfected with indicated plasmids. Protein lysates were evaluated by western-blot.

(C and D) HEK29T cells were co-transfected with Myc-USP21 (USP21) or an empty Myc-vector (Myc) and Flag-Gli1 or -Gli2 or an empty Flag-vector (Flag). Cells were lysed in NP40-lysis buffer and subjected to immunoprecipitation with anti Flag M2 affinity gel (C) or anti-Myc antibody (D), followed by western blotting with indicated antibodies.

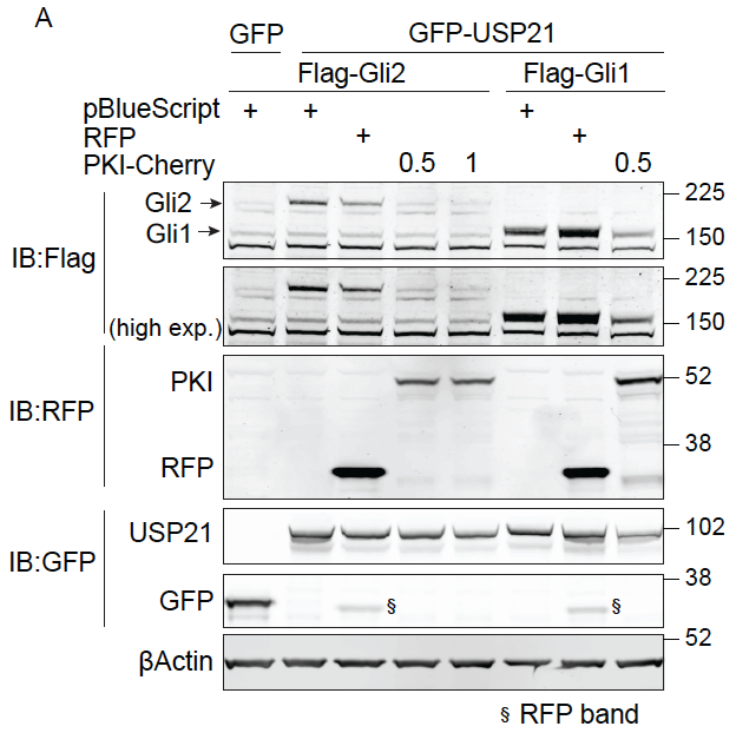

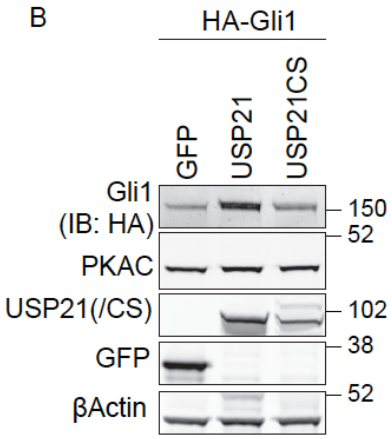

Supplementary Figure 4: USP21 promotes Gli1 and Gli2 phosphorylation by PKAC without affecting PKAC expression levels.

(A) USP21 promotes Gli2 phosphorylation by PKAC. HEK293T were transfected with Flag-Gli1 or Flag-Gli2, GFP or GFP-USP21 and increasing amounts (µg) of PKI-Cherry or RFP control plasmids. Cells were lysed 24h after transfection. Samples were assessed by western-blotting with Flag and RFP antibodies and membranes reprobed with anti-GFP. High exp. : high exposure.

(B) USP21 overexpression does not affect PKA protein levels. HEK293T cells were transfected with indicated plasmids. Protein lysates were evaluated by western-blot.